A Nine-Noded Quadratic Control-Volume-Based Finite Element for Heat Conduction

M.J. Raw,* G.E. Schneider,† and V. Hassani‡
University of Waterloo, Waterloo, Ontario, Canada

A control-volume-based finite element formulation is presented for the nine-noded, quadratic, quadrilateral finite element for application to conduction heat transfer. The formulation is presented with the nine-noded element being used rather than the eight-noded element for reasons of convenience of control volume definition. The quadratic nature of the element in itself offers greater geometric flexibility and the potential for significantly higher accuracy than does the previous linear control volume element. It was observed that for steady-state conduction, the central control volume 'numerical molecule' is the optimal, fourth order operator on a uniform grid; however, due to the large connectivity for the corner control volume, such a 'molecule' interpretation is not readily facilitated. Performance of the element was evaluated through application to two test problems. It was observed that on the predominantly flux prescribed problem the performance is comparable to that of the Galerkin formulation. However, for the Dirichlet problem, a reduction of error by two orders of magnitude over the Galerkin formulation was observed.

Nomenclature

a,b	= test case dimensions
c	= specific heat, or test case dimension
C	= boundary condition constant
E	= total control volume energy
h	= heat transfer coefficient
i,j	= unit vectors in x,y directions
J	= Jacobian of transformation matrix
$k_{i,j}$	= coefficient in stiffness matrix
k_x,k_y,k_n	= conductivity in x,y,n, directions
n	= normal
N_i	= shape function
p	= heat generation per unit volume
P	= total control volume heat generation rate
q	= heat flux
Q	= heat flow rate
r_i	= right hand side of algebraic equation system
s	= local coordinate
S	= surface
t	= local coordinate or time
T	= temperature
V	= volume
x,y	= Cartesian coordinates
ρ	= density

Introduction

THE need for discrete methods in the modeling of physical systems has long been recognized by the engineering and scientific community. The application of discrete methods to the solution of physical problems effectively began when Richardson[1] presented his paper to the Royal Society. In his first approximate procedures, his efforts were directed at determining an approximate representation of the governing equation, rather than at obtaining an approximation to the particular balance represented by the equation. Approximations for derivatives were obtained from truncated Taylor Series expansions of the dependent variable in the vicinity of the point of interest. Consequently, this form of the method of finite differences has become known as a Taylor Series formulation. While this form of the finite difference method has historically been restricted to rectangular domains and meshes, Schneider, Strong and Yovanovich[2] extended the method to include applicability to general, orthogonal, curvilinear coordinate systems. More recently, Robertson[3] applied the Taylor Series approach to problems involving general, non-orthogonal, curvilinear coordinate systems.

A control volume approach to the discrete modeling of physical systems is gaining considerable popularity among contemporary heat transfer analysts and researchers,[4] however, and entails applying an energy balance directly to the discrete control volumes comprising the domain. Only where control volume surface fluxes require approximation are Taylor Series representations employed. As a result of this approach, the control volume formulations enjoy the desirable properly of being conservative; that is, the discrete equations maintain an accurate accounting of the energy flows through the domain by ensuring that the approximation for these surface fluxes is unique and independent of the side from which the surface is viewed. This approach has been extended to general, orthogonal, curvilinear coordinate systems by Schneider, Strong and Yovanovich,[5] and, more recently, to general nonorthogonal, curvilinear coordinate systems by Zedan and Schneider.[6]

In the application of the above procedures, however, it is paramount that the coordinate system be defined over the entire solution domain. Examples of application of these procedures have been provided for the more exotic orthogonal systems,[2,5] analytically defined nonorthogonal coordinate systems[3,6] and systems obtained as the result of a numerical coordinate transformation.[7] The disadvantage of these procedures is that the coordinate system must be defined, a priori, over the entire solution domain, and this detracts significantly from the flexibility of the methods. Finite element methods, while geometrically flexible, have followed a philosophically different approach from that followed by finite difference methods. In stress analysis, a variational extremum principle can be employed which naturally leads to the formulation of a discrete model. Conversely, in conduction heat transfer and convective transport problems such a natural formulation having a clear physical basis does not exist. Although several quasi or pseudovariational formulations have been proposed,[8,9,10] the Galerkin method[11] is more frequently employed by contemporary researchers to formulate finite element models for heat conduction problems. The resulting equations, however, are nonconservative in nature, and direct

Presented as Paper 84-0493 at the AIAA 22nd Aerospace Sciences Meeting, Reno, Nev., Jan. 9-12, 1984; submitted March 1, 1984; revision submitted Sept. 13, 1984. This paper is declared a work of the Canadian Government and therefore is in the public domain.

*Graduate Student, Department of Mechanical Engineering. Member AIAA.

†Professor, Department of Mechanical Engineering. Member AIAA.

‡Graduate Student, Department of Mechanical Engineering.

control of the energy flow is therefore precluded from the user.

Baliga and Patankar,[12] through the use of specialized interpolation functions, have proposed a control-volume-based finite element procedure for convection-diffusion problems. Their procedure, however, is applicable only to linear triangular elements. More recently, Schneider and Zedan[13] have propsed a control-volume-based finite element method for conduction heat transfer in which there are no intrinsic restrictions on element shape or interpolation order. In their paper, a control volume balance approach was implemented starting with a single, linear, quadrilateral element comprising four sub-control-volumes. For each or these sub-control-volumes, heat flows at their surfaces were defined in order to effect the energy balance. The internal heat flows were expressed in terms of nodal temperatures, through the conventional use of shape functions, while external flows were resolved through an appropriate assembly rule or through application of boundary conditions where appropriate. It was shown that the resulting 'numerical molecule' more closely reflects the expected physical behavior of the system than does that resulting from the conventional formulation. The paper by Schneider and Zedan,[13] therefore, has laid the basis for more extensive application of a control volume formulation of the finite element equation governing physical systems.

It is the purpose of the present paper, therefore, to start from the previous work of Schneider and Zedan, and extend the control-volume-based finite element formulation for conduction heat transfer problems to the nine-noded, isoparametric, quadratic, quadrilateral finite element. This element possesses the desirable attribute of greater flexibility in describing bodies having curved as well as straight boundary geometrics and also has the potential for enhanced accuracy due to the quadratic nature of the interpolation. The extension of control-volume-based finite element principles to this element is therefore seen as a significant contribution to the state-of-the-art of discrete methods. This work is also viewed as a further step in the continuing evolution towards a marriage between finite difference and finite element methods in which the most desirable attributes of each of these methods are retained in their union.

Geometric Preliminaries

A typical problem domain is illustrated in Fig. 1a where it could be interpreted as a quadrant of a model for determining the heat loss from a cylindrical flue through a rectangular section to an ambient environment. In this application, the use of quadratic elements will be useful to describe the circular cross-section of the inner surface. A general quadratic, quadrilateral, isoparametric finite element is shown in Fig. 1b where the location of the nodes, their numbering sequence, and the local (s,t) coordinate system are shown. The midside and central nodes are located at locations corresponding to $s=0$ or $t=0$ as appropriate. The temperature field and the global coordinates (x,y) are given in conventional form according to[14]

$$T=\sum_{j=1}^{9} N_j T_j \tag{1}$$

$$x=\sum_{j=1}^{9} N_j x_j \tag{2}$$

$$y=\sum_{j=1}^{9} N_j y_j \tag{3}$$

where the shape functions, N_j, are given by

$$N_1 = st(1+s)(1+t)/4 \tag{4a}$$

$$N_2 = -st(1+s)(1-t)/4 \tag{4b}$$

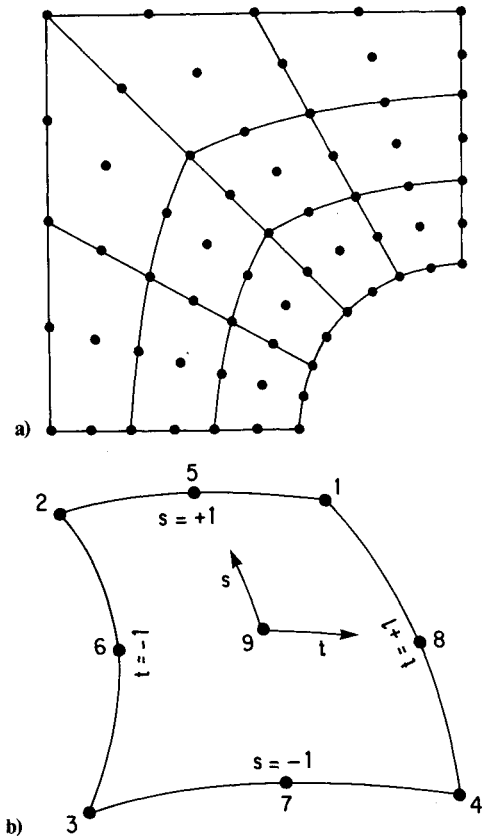

Fig. 1 Finite element mesh with a) typical grid distribution and b) a single element.

$$N_3 = st(1-s)(1-t)/4 \tag{4c}$$

$$N_4 = -st(1-s)(1+t)/4 \tag{4d}$$

$$N_5 = s(1+s)(1+t)(1-t)/2 \tag{4e}$$

$$N_6 = -t(1+s)(1-s)(1-t)/2 \tag{4f}$$

$$N_7 = -s(1-s)(1+t)(1-t)/2 \tag{4g}$$

$$N_8 = t(1+s)(1-s)(1+t)/2 \tag{4h}$$

$$N_9 = (1+s)(1-s)(1+t)(1-t) \tag{4i}$$

From the expression for temperature, Eq. (1), the x and y derivatives can be determined as

$$\frac{\partial T}{\partial x}=\sum_{j=1}^{9}\frac{\partial N_j}{\partial x}T_j \tag{5}$$

$$\frac{\partial T}{\partial y}=\sum_{j=1}^{9}\frac{\partial N_j}{\partial y}T_j \tag{6}$$

with the x and y derivatives of the shape functions appearing in Eqs. (5) and (6) determined in the usual fashion by

$$\begin{Bmatrix} \dfrac{\partial N_j}{\partial x} \\ \dfrac{\partial N_j}{\partial y} \end{Bmatrix} = \frac{1}{\mathrm{Det}[J]} \begin{bmatrix} \dfrac{\partial y}{\partial t} & \dfrac{-\partial y}{\partial s} \\ \dfrac{-\partial x}{\partial t} & \dfrac{\partial x}{\partial s} \end{bmatrix} \begin{Bmatrix} \dfrac{\partial N_j}{\partial s} \\ \dfrac{\partial N_j}{\partial t} \end{Bmatrix} \tag{7}$$

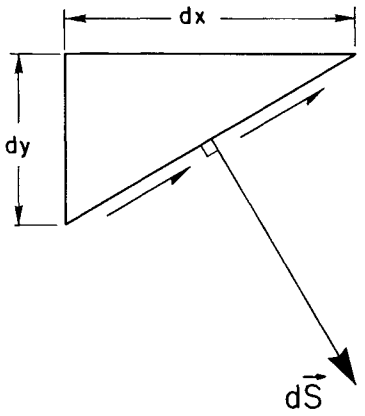

Fig. 2 Surface line segment and normal.

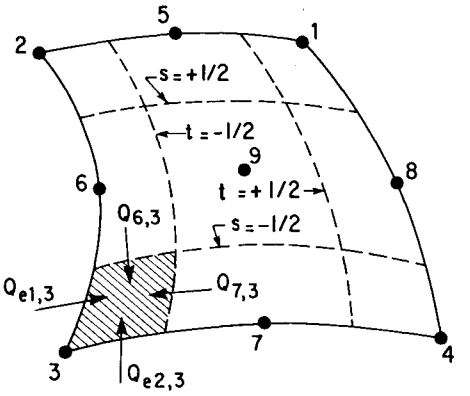

Fig. 3 Single element with control volume subdivision and heat flows.

where

$$\text{Det}[J] = \frac{\partial x}{\partial s}\frac{\partial y}{\partial t} - \frac{\partial y}{\partial s}\frac{\partial x}{\partial t} \tag{8}$$

Finally, considering the general line segment shown in Fig. 2, being traversed in the direction shown by the arrow, the outward normal, $d\vec{S}$, can be expressed in the form

$$d\vec{S} = dy\hat{i} - dx\hat{j} \tag{9}$$

The outward normal defined in this manner is consistent with the convention of counter-clockwise surface integration taken to be positive.

Element Property Equations

Following a procedure analogous to that proposed by Schneider and Zedan[13] for the linear quadrilateral, a single, isolated, finite element will be first considered. This will permit the element matrix equations, which express the nodal temperature vs nodal heat flow relationships, to be determined. The assembly process will then be used to construct the global equation system from the elemental equations.

To derive the elemental equations, the isolated finite element illustrated in Fig. 3 is considered. In this figure, the element is subdivided into nine internal control volumes, each of which can be associated with a corresponding node of the element definition vector. Indeed, it is the requirement for subdivision into internal control volumes that prompts the use of the nine-noded quadratic element rather than the use of the more frequently encountered eight-noded quadratic element. In adopting a control-volume-based formulation, it is necessary to establish these control volumes and their defining surfaces. The use of thes nine-noded element provides a convenient mechanism to achieve this definition. The control volume surfaces utilized in this paper are delineated by lines of constant s and t having values of -0.5 and $+0.5$ for each. In this way, nine subcontrol volumes are readily identified, as shown in the figure, and further, through the above defining surface selection, the global control volumes, formed as a result of the assembly process, will be of equal extent, in terms of their s and t coordinate range and will be of equal size in a uniform mesh environment. Also, this choice satisfies the essential requirement that control volume surfaces remain continuous after assembly.

In words, an energy balance applied to a single control volume can be expressed as

[Net rate of conduction into control volume]

+ [Rate of generation within control volume]

= [Rate of change of energy within control volume] (10)

Referring specifically to control volume 3 of Fig. 3, this equation has mathematical representation as

$$Q_{6,3} + Q_{7,3} + Q_{e1,3} + Q_{e2,3} + \iint_{\text{C.V.}} p\,dV = \frac{\partial}{\partial t}\iint_{\text{C.V.}} \rho c T\,dV \tag{11}$$

where the integration limits are those corresponding to the control volume associated with node 3. The subscripts *el* and *e2* in Eq. (11) refer to energy flows into control volume 3 through surfaces which are on the exterior of the element and which emanate from either the physical domain boundary or from adjacent elements, and these energy flows will be considered when the assembly procedure and boundary condition application are considered. Further, it is noted that control volumes 5, 6, 7, and 8 have only one such external heat flow while control volume 9 has no external heat flows. However, volumes 5, 6, 7, and 8 have three internal heat flows requiring evaluation while control volume 9 has the requirement for four internal heat flow evaluations. Indeed, it is far more convenient, from coding considerations, to consider each of the internal heat flows in turn and their appropriate control volume contributions than to complete the assembly of any given control volume. The coding necessary to effect this is direct and straightforward. In addition, it is noted that many of the control surfaces and volumes not only have differing limits of integration but also have differing ranges of integration with respect to the s and t (and global) coordinate frame. Nevertheless, these considerations are also readily implemented.

The internal heat flows involved in Eq. (11) are calculated according to the general relation

$$Q = -\int_s \vec{q}\cdot d\vec{S} \tag{12}$$

where the heat flux vector is given by

$$\vec{q} = -k_x\frac{\partial T}{\partial x}\hat{i} - k_y\frac{\partial T}{\partial y}\hat{j} \tag{13}$$

and the element of surface, dS is determined using Eq. (9). The algebraic, calculus, and manipulation details necessary to complete the representation of the energy balance equation given by Eq. (11) are similar in every respect to those presented in the earlier paper by Schneider and Zedan[13] for the linear quadrilateral element. The reader is referred to that paper in which the derivation is presented for that element. The final result, at element level for control volume 3, can be represented in the form

$$\sum_{j=1}^{9} k^{e,*}_{3,j}\, T^e_j = r^{e,*}_3 \tag{14}$$

where the coefficients and right hand side for control volume 3 are given by

$$k^{e*}_{3,j} = -\int_{-1}^{-0.5}\left[k_x\frac{\partial N_j}{\partial x}\frac{\partial y}{\partial s} - k_y\frac{\partial N_j}{\partial_y}\frac{\partial x}{\partial s}\right]\Big|_{t=0.5} ds + \int_{-1}^{-0.5}\left[k_x\frac{\partial N_j}{\partial x}\frac{\partial y}{\partial t} - k_y\frac{\partial Nj}{\partial_y}\frac{\partial x}{\partial t}\right]\Big|_{s=-0.5} dt + \frac{1}{\Delta t}\int_{-1}^{-0.5}\int_{-1}^{-0.5}\rho c N_j\,|\mathrm{Det}\,[J]|\,ds\,dt \quad (15)$$

and by

$$r^{e*}_3 = \int_{-1}^{-0.5}\int_{-1}^{-0.5} p\,|\mathrm{Det}\,[J]|\,ds\,dt + \sum_{j=1}^{9}\left\{\frac{1}{\Delta t}\int_{-1}^{-0.5}\int_{-1}^{-0.5}\rho c N_j\,|\mathrm{Det}\,[J]|\,ds\,dt\right\}T^0_j + (Q_{el,3}+Q_{e2,3}) \quad (16)$$

In the above, the superscript e denotes that the indicated terms have been evaluated from elemental consideration. Equations similar to Eq. (14) can be written for the remaining control volumes although the limits of the surface integration and the corresponding sign of the integral will vary depending on the particular control volume under consideration. Further, the reader is reminded that $Q_{i,j} = Q_{j,i}, i \neq j$, and that considerable computational savings as well as a reduction in complexity will result if heat flows are evaluated term by term with an ensuing contribution addition to the terms representing the control volume energy balance. It remains to assemble the element stiffness matices to form the global system of equations and to facilitate the implementation of boundary conditions.

Assembly Procedures and Boundary Condition Application

The assembly rules and the mechanism for boundary condition implementation are also very closely aligned with those employed for the linear quadrilateral element examined by Schneider and Zedan.[13] Within the interior of the domain, the elementally external heat flows, $Q_{el,3}$ and $Q_{e2,3}$ for example, represent heat flows into the control volume from regions external to the element. It is recognized the adjacent internal elements will contain similar terms at their boundaries and that the sum of all heat flows at common boundaries must be supplied externally. The assembly process then simply equates their sum to the externally applied heat flow, and for continuum problems, this sum is set to zero. In practice, however, this is accomplished by not considering their evaluation at all within the interior. This procedure applies for all interior element boundaries irrespective of whether the associated control volume is a corner volume or a midsize volume. For the central volume, control volume 9, these external heat flows never appear in the formulation.

The assembly procedure then results in the accumulation of adjacent subcontrol volumes into larger volumes over which the actual energy balance is being affected. Figure 4 indicates the three control volume types which result due to the assembly of corner or midside control volumes, or simply to the unaffected central control volume. At element boundaries, however, the conservation constraint is applied to the subcontrol volumes directly with the help of boundary condition application considered below. This accumulation of subcontrol volumes into larger control volumes is analogous to the 'domain of influence' resulting from the assembly of conventional finite elements. Indeed, the extent of the domain of influence for the control-volume-based formulation is less than that of the conventional formulation wherein an overlapping of adjacent domains of influence occurs.

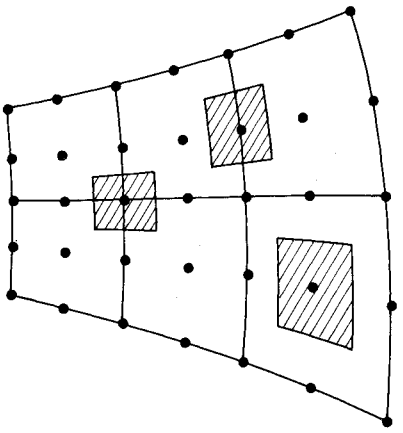

Fig. 4 Three different effective control volumes resulting from the assembly process.

For element subcontrol volumes which lie on a physical boundary of the domain, the above cancellation of externally applied heat flows does not occur. However, it is precisely those heat flows which do not cancel which provide the mechanism for boundary condition implementation. The boundary condition which is considered is the general convective condition given by

$$k_n\frac{\partial T}{\partial n} + \mathrm{h}T = \mathrm{C} \quad (17)$$

which, through appropriate selection of the constants h and C, can be used to describe a Neumann boundary condition and a Dirichlet boundary condition as well as the actual convective boundary condition. Again the procedure is entirely analogous to that employed for the linear quadrilateral by Schneider and Zedan[13] and for the details of the derivation the reader is referred to that paper. After application of boundary conditions, the equation representing an energy balance for control volume 3 can be written as

$$\sum_{j=1}^{9} k^e_{3,j}T^e_j = r^e_3 \quad (18)$$

where

$$k^e_{3,j} = -\int_{-1}^{-0.5}\left[k_x\frac{\partial N_j}{\partial x}\frac{\partial y}{\partial s} - k_y\frac{\partial N_j}{\partial y}\frac{\partial x}{\partial s}\right]\Big|_{t=0.5} ds + \int_{-1}^{-0.5}\left[k_x\frac{\partial N_j}{\partial x}\frac{\partial y}{\partial t} - k_y\frac{\partial N_j}{\partial y}\frac{\partial x}{\partial t}\right]\Big|_{s=0.5} dt + \frac{1}{\Delta t}\int_{-1}^{-0.5}\int_{-1}^{-0.5}\rho c N_j\,|\mathrm{Det}\,[J]|\,ds\,dt + \int_{S_3} hN_j\,dS_3 \quad (19)$$

$$r^e_3 = \int_{-1}^{-0.5}\int_{-1}^{-0.5} p\,|\mathrm{Det}\,[J]|\,ds\,dt + \sum_{j=1}^{9}\left\{\frac{1}{\Delta t}\int_{-1}^{-0.5}\int_{-1}^{-0.5}\rho c N_j\,|\mathrm{Det}\,[J]|\,ds\,dt\right\}T^0_j + \int_{S_3} \mathrm{C}\,dS \quad (20)$$

where the surface integrals are evaluated only when the surface coincides with the physical domain boundary and for all surfaces on the domain boundary. It is noted, consistent with conventional finite element formulations, that an adiabatic boundary condition is effected by default if no action is taken regarding the above exterior integrals. Thus, the 'natural' boundary condition remains an adiabatic condition. All integrations were evaluated numerically using a sufficiently high

order quadrature that, on the basis of quadrature order studies, the integrations were exact to six significant digits.

It is common practice to examine the numerical molecule that results from the assembly of elements having a common node. However, in the case of the nine-noded quadratic quadrilateral, two complications arise. First, there are three different molecules that result from the assembly of the three different types of subcontrol volume: the corner, midside, and central subcontrol volumes. Second, the connectivity is extensive, particulary for the corner, with 25 temperatures involved in general in the conservation equation. Thus a detailed description of the resulting 'numerical molecule' will not be provided. However, it is worthy of note that the central subcontrol volume has a connectivity of 9 and that its 'numerical molecule' representation is highly accurate. Indeed, the 'numerical molecule' corresponding to this subcontrol volume has a relative weighting for a regular mesh of 1.0 for the corner temperatures, 4.0 for side temperatures, and 20 for the central temperature, for the case of steady-state, isotropic and uniform conductivity, configuration. This molecule corresponds to the optimal, fourth order accurate representation of the Laplacian.[12] This is indeed a highly encouraging result.

Application to Test Problems

The nine-noded, quadratic, quadrilateral control-volume-based formulation was coded and tested to validate the formulation. On the basis of the success achieved with the linear quadrilateral control volume formulation by Schneider and Zedan,[13] no difficulties were anticipated insofar as operation of the procedure was concerned. The purpose of the testing, therefore, is to provide a qualitative measure of the expected performance of the nine-noded control volume formulation when compared with that of the more conventional Galerkin formulation.

Following code validation on various one-dimensional problems, two specific test cases were examined as illustrated in Fig. 5. The two test cases are both rectangular in domain shape for ease in grid generation and, in the first case, for ease of generation of an analytic solution for comparison. However, the boundary condition specifications[5] of the two test cases are quite different. In the first case, the upper surface is convectively coupled to an ambient fluid through a film coefficient with a portion of the lower surface exposed to a uniform flux application. The remaining domain boundary is adiabatic. The second test case is subjected to a Dirichlet boundary specification over the entire boundary. For each of the two test cases, two parameter combinations were employed with steady-state, zero source strength conditions prevailing for both.

For the first case the geometric and thermal configuration is illustrated in Fig. 5a, with the specific parameters employed for the two configurations of this test case presented in Table 1. The analytical solution for this problem is available as determined by Schneider, Yovanovich, and Cane.[16] For configuration one of test case 1, the maximum temperature error of the conrol volume formulation was .27% while for the Galerkin formulation the maximum temperature error was 0.33%. An rms error was also determined based on nodal point errors. It is noted that the errors are normalized with respect to the maximum range in temperature over the domain. The rms error for the control volume formulation was 0.11% while that for the Galerkin formulation was 0.10%. Thus while the rms errors are effectively the same, the control volume formulation provided a slightly lower maximum error. The error at two different y locations is presented in Fig. 6. It is seen from this figure that, at both $y=0.0$ and $y=0.05$, the error distributions of the two formulations are very similar. However, it is observed that the oscillations resulting in the vicinity of the region of flux application are more pronounced for the Galerkin formulation. Even at $y=0.05$, i.e. half-way across the thickness, the Galerkin formulation retains significant oscillations while the control volume formulation has a more smoothly varying error distribution. Nevertheless, it can be concluded that the performance of the two formulations are very similar for this configuration. The second configuration of test case 1, with parameters as presented in Table 1, supports this observation producing a maximum and rms error of 0.156 and 0.0312% for the control volume formulation, and 0.132 and 0.0179%, respectively, for the Galerkin formulation. For this type of problem specification, therefore, the two formulations have very similar performance characteristics, and, as witnessed by the high accuracy for the relatively crude meshes employed, both demonstrate very good performance.

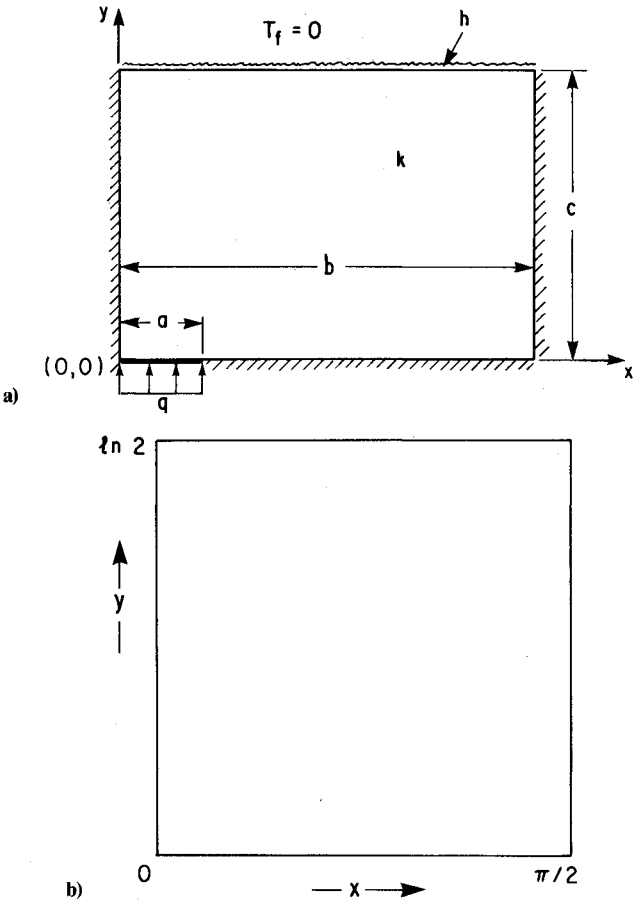

Fig. 5 Two test cases used for evaluation of procedure.

Table 1 Test case 1 parameters

Configuration	a	b	c	h	Tf	Elements (x^*y)
1	0.2	1.0	0.1	1.0	0.0	10×5
2	0.5	1.0	1.0	∞	0.0	6×6

The second test case, that having Dirichlet conditions specified over the entire boundary, produced dramatically different results in a comparative sense. Again two specific configurations were examined and the appropriate parameters are presented in Table 2. The temperature distributions indicated in Table 2 were selected since they inherently satisfy Laplace's equation. Further, the horizontal variation is such that in configuration one a smooth sinusoidal variation is observed starting at 0 at $x=0.0$ and having its only maximum at the right hand boundary where $x=\pi/2$. The second configuration again begins at 0 at $x=0.0$, but peaks at $x=\pi/2$. The vertical domain extent is from $y=0$ to $y=\ell n2$.

For this second test case, the control volume formulations yield highly superior results. For configuration one, for exam-

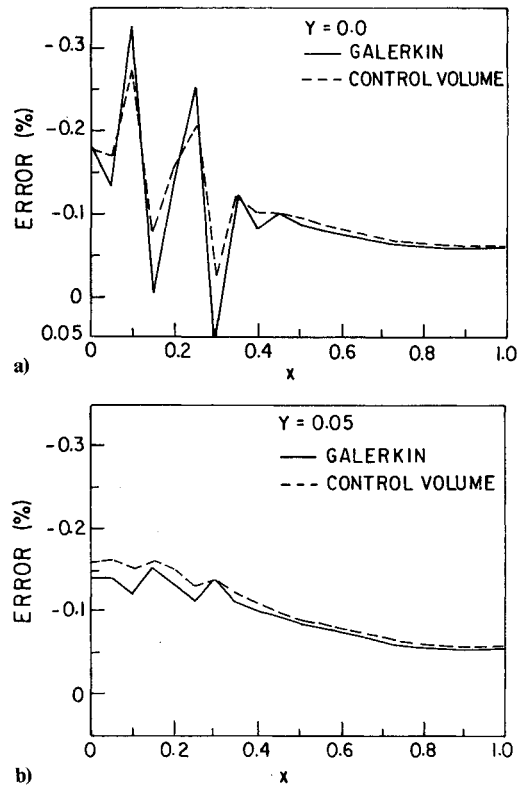

Fig. 6 Error distribution comparison for test case 1.

Table 2 Test case 2 parameters

Configuration	Temperature specification	Elements (x^*y)
1	$T=\sin\times e^{y}$	4×4
2	$T=\sin 2\times e^{2y}$	4×4

ple, the Galerkin formulation resulted in maximum and rms errors of 0.697 and 0.151%, respectively. Conversely, using the control volume formulation, the corresponding maximum and rms errors were 0.002 and 0.00072%! Such a high accuracy is indeed surprising since the computations were themselves performed in single precision on an IBM 4341 installation. The analytic values, however, were computed in full double precision. The error distribution for test case 2, configuration one, is presented in Fig. 7, where the abscissa represents distance along the diagonal from (0,0) to ($\pi/2$, ℓn 2). On the scale of the figure, the control volume error is essentially a straight line having effectively zero error. Conversely, while the Galerkin formulation yields acceptable results in the central region, both ends demonstrate an increase in error. Indeed, relative to the control volume error distribution, the Galerkin formulation error distribution exhibits large oscillations near location ($\pi/2$, $\ell n 2$). For this case the improvement in maximum error using the control volume formulation is a factor of 348 while the improvement in the rms error is a factor of 209. These results are supported by the second configuration of test case 2. For this case, the Galerkin formulation yielded a maximum and rms error of 2.8 and 0.55%, respectively, while the control volume formulation yielded a maximum and rms error of 0.03 and 0.012%, respectively.

It appears, then, that while the control volume and Galerkin formulations yield comparable performance for the predominantly flux specified problem, the control formulation offers a dramatic improvement in performance for the Dirichlet specified problem.

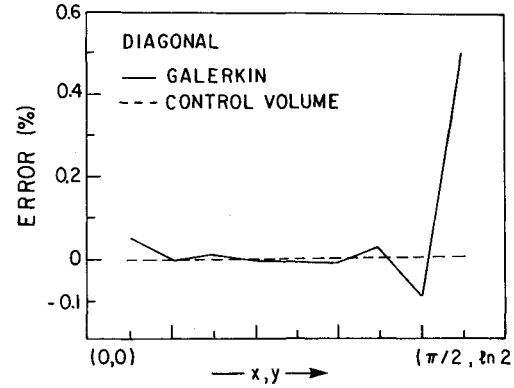

Fig. 7 Error distribution comparison for test case 2.

Discussion and Conclusions

A control volume finite element formulation has been presented for the nine-noded, quadratic, quadrilateral finite element for the modelling of diffusion problems. The motivation for examining the control volume formulation for the nine-noded element has been fourfold. First, it was deemed important to gain additional experience with control volume formulations in a finite element environment since this concept is relatively new. Secondly, it is desirable to expand the repertoire of control volume finite elements available to the analyst, particularly since the nine-noded element offers considerable potential for enhanced geometric description and for improved accuracy over the linear quadrilateral. Thirdly, it was important to acquire additional quantitative data relative to the performance of control-volume-based finite element formulations. Finally, this work represents the continuation of an effort to form a marriage between the finite element and finite difference methods, wherein the more desirable features of both methods coexist in their union.

It was demonstrated that the procedures involved in extending the control volume formulation to the nine-noded element follow naturally from the concepts advanced in the original linear quadrilateral element. The only constraint employed in the quadratic case was the use of nine nodes, instead of the eight-noded quadratic element, and this constraint was introduced primarily for reasons of convenience in defining control volume configurations. The fact that the original concepts for a control volume formulation can be so readily adapted to other element configurations is a significant conclusion of this work.

The performance of the nine-noded, quadratic, quadrilateral control-volume-based finite element formulation was evaluated by application to two test problems, for each of which two configurations were examined. It was observed that, although for the predominantly flux prescribed problem the performance of the control volume formulation and of the Galerkin formulation were essentially identical, the Dirichlet problem resulted in a drastic improvement of the control volume formulation over the Galerkin formulation. Reductions in error in the temperature field, on both a maximum and *rms* basis, of two orders of magnitude were observed. Aside from the computational advantages resulting from the procedure, of course, there is the direct benefit that conservation is guaranteed, both locally and globally.

Acknowledgments

The authors express their appreciation to the Natural Sciences and Engineering Research Council of Canada for their financial support of this project in the form of an operating grant to G.E. Schneider.

References

[1]Richardson, L.F., "The Approximate Arithmetical Solution by Finite Differences of Physical Problems Involving Differential Equations, with an Application to the Stresses in a Masonry Dam," *Transactions of the Royal Society of London,* Series A. Vol. 120, 1910, pp. 307-357.

[2]Schneider, G.E., Strong, A.B., and Yovanovich, M.M, "Finite Difference Modelling of the Heat Conduction of Equation in General Equation Orthogonal Curvilinear Coordinates Using Taylor Series Expansion," *Proceedings of the Association International pour les Computation Analogique International Symposium on Computer Methods for Partial Differential Equations*, edited by R. Vichnevetsky, Lehigh University, Bethlehem, Pa., June 1975, pp. 312-317.

[3]Robertson, S.R., "A Finite Difference Formulation of the Equation of Heat Conduction in Generalized Coordinates," *Numerical Heat Transfer,* Vol. 2, 1979, pp. 61-80.

[4]Patankar, S.V., *Numerical Heat Transfer and Fluid Flow,* McGraw-Hill Book Co., New York, 1980.

[5]Schneider, G.E., Strong, A.B., and Yovanovich, M.M, "A Physical Approach to the Finite Difference Solution of the Conduction Equation in Orthogonal Curvilinear Coordinates," ASME Paper 75-WA/HT-94, 1975.

[6]Zedan, M., and Schneider, G.E., "A Physical Approach to the Finite Difference Solution of the Conduction Equation in Generalized Coordinates," *Numerical Heat Transfer,* Vol. 5, 1982, pp. 1-19.

[7]Thompson, J.F., Thames, F.C., and Mastin, C.W., "Automatic Numerical Generation of Body-Fitted Curvilinear Coordinate System for Field Containing Any Number of Arbitrary Two-Dimensional Bodies." *Journal of Computional Physics,* Vol. 15, 1974, pp. 299-319.

[8]Zrenkicwicz, O.C., and Parekh, C.J., "Transient Field Problems: Two-Dimensional and Three-Dimensional Analysis by Isoparametric Finite Elements," *International Journal for Numerical Methods in Engineering,* Vol. 2, 1970. pp. 61-74.

[9]Zienkiewicz, O.C., *Finite Elements in Engineering Science,* McGraw-Hill Book Co., 1971.

[10]Biot, M.A., "Variational Principles in Irreversible Thermodynamics with Applications to Viscoelasticity," *Physical Review,* Vol. 97, No. 6, 1955, pp. 1463-1469.

[11]Finlayson, B.A., and Scriven, L.E., "On the Search for Variational Principles," *International Journal for Heat and Mass Transfer,* Vol. 10, 1967, pp. 799-821.

[12]Baliga, B.R., and Patankar, S.V., "A New Finite Element Formulation for Convection-Diffusion Problems," *Numerical Heat Transfer,* Vol. 3, No. 4, 1980. pp. 393-409.

[13]Schneider, G.E., and Zedan, M., "Control Volume Based Finite Element Formulation of the Heat Conduction Equation," *Spacecraft Thermal Control, Design, and Operation,* Progress in Astronautics and Aeronautics, Vol. 86, edited by H.E. Collicott and P.E. Bauer, AIAA, New York, 1983, pp. 305-327.

[14]Huebner, K.H., *The Finite Element Method for Engineers*, John Wiley and Sons, New York, 1975.

[15]Greenspan, D. "On a 'Best' 9-Point Different Equation Analog of Laplace Equation," *Journal of the Franklin Institute,* Vol. 263, 1967, pp. 425-430.

[16]Schneider, G.E., Yovanovich, M.M. and Cane, R.L.D., "Thermal Constriction Resistance of a Convectively Cooled Plate with Non-Uniform Flux Over its Opposite Face," *Journal of Spacecraft and Rockets,* Vol. 17, July-Aug. 1980, pp. 372-376.